Hittite Journal of Science and Engineering, 2017, 4(2) 117-123
ISSN NUMBER: 2149-2123
DOI: 10.17350/HJSE19030000057

Optical sensing of mercury using fluorescent silver and gold nanoclusters

Mehmet Gökhan Çağlayan
Ankara University, Faculty of Pharmacy, Department of Analytical Chemistry, Ankara, TURKEY

ABSTRACT

In this study, gold and silver nanoclusters were employed for optical sensing of mercury. Nanoclusters used in this research had different chemical properties and showed different interactions with mercury producing specific optical responses including UV-Vis absorbance and fluorescence. These responses were quantitatively studied in the solution phase. The sensitive methods developed in this study were tested using mercury standards and accurate and precise results were obtained. Optical responses could also be monitored by naked eye. Finally, portable and simple glass fiber pads were developed for mercury sensing.

Article History:
Received : 2017/07/24
Accepted: 2017/08/25
Online : 2017/10/17

***Correspondence to**: Mehmet Gökhan Çağlayan, Ankara University, Faculty of Pharmacy, Department of Analytical Chemistry, Ankara, TURKEY*
E-Mail: gcaglayan@ankara.edu.tr

Keywords:
Mercury sensing, optical sensors, gold nanoclusters, silver nanoclusters, fluorescence, colorimetry, portable optical devices

INTRODUCTION

Mercury has neurotoxic, teratogenic, nephrotoxic and immunotoxic effects on human health [1-3]. Humans are exposed to mercury from different sources such as release from dental amalgams, gold mining activities, application of thiomersal-containing vaccines and industrial discharge to the environment [4]. Although mercury pollution is rare compared to other types of pollutions, it is strictly followed in environmental samples such as seawater and drinking water and is restricted by national and international regulations due to its hazardous effects on the ecosystem and human health. According to the Ministry of Health of Turkey, the concentration of mercury in drinking water must not exceed 1 μg/L (~5 nM) and the limit defined by the United States Environmental Protection Agency is 2 μg/L (~10 nM). Such a low amount of mercury can generally be analyzed only by highly sensitive analytical techniques such as inductively coupled plasma, mass spectrometry [5-6] fluorescence sensing [7-8], high performance liquid chromatography, cold vapor atomic fluorescence spectroscopy [9], and resonance Rayleigh scattering aptasensors [10].

Although developing a method for any forms of mercury is worthwhile, all Hg forms produce Hg^{2+} and most studies have focused on the development of mercury sensors through Hg^{2+} sensing [4,11-13]. Recently, a considerable number of nanoparticle-based sensors for ultra-sensitive analysis have been developed due to the lower cost and versatile and modifiable features of these materials and the simplicity of their synthesis and analysis [12-13]. There are different mechanisms for Hg nanosensing and the easiest is the aggregation of nanoparticles in the presence of Hg^{2+} [14]. Silver nanoparticles result in the reduction of Hg^{2+} and an Hg-Ag amalgam can be formed on the surface of nanoparticles when the size of the silver nanoparticles are below 32 nm [15]. When this occurs, optical responses such as shifting surface plasmon resonance (SPR) bands and fluorescence quenching can be observed. Another strategy is based on the affinity of thymine to Hg^{2+} ions [16], in which the thymine-thymine mismatched base pair is stabilized by Hg^{2+} with a size that perfectly fits the double stranded DNA without the steric disturbance of the helical structure. Other mechanisms in fluorescence nanosensing include energy transfer and electron transfer between analytes and sensors.

There are various types of luminescent nanomaterials that can be used in optical sensing of analytes and they introduce different mechanisms in sensing methods. The most employed luminescent particles in nanosensing are quantum dots [7,17]. Recently, as an alternative to quantum dots, nanoclusters of noble metals have been employed in this area [18].

Gold nanoclusters (AuNC) and silver nanoclusters (AgNC) are preferred particularly due to their easy synthesis, biocompatibility, and photostability.

In this study, AgNC and AuNC were used for Hg^{2+} sensing. Their fluorescence and absorbance signals were monitored after the addition of Hg^{2+}. Finally, the method was transferred to glass fiber pads for a simple and on-site analysis of Hg^{2+}.

METHOD

Materials and instrumentation

NaOH, $HAuCl_4$, $Hg(NO_3)_2$, $NaBH_4$, KNO_3, $NaNO_3$, $Ca(NO_3)_2$, $Fe(NO_3)_2$, $Mg(NO_3)_2$, $Ba(NO_3)_2$, $Pb(NO_3)_2$, α-Lipoic acid, L-glutathione, and Whatman No 1 Chr chromatography paper were purchased from Sigma-Aldrich (Mannheim, Germany). Mercury reference standard was purchased from Ultra Scientific Analytical Solutions (Rhode Island, USA). Glass fibers conjugate pad sheets and absorbent pads were obtained from Merck Millipore (Darmstadt, Germany).

Fluorescence spectra were measured with an Agilent Cary Eclipse Fluorescence Spectrophotometer and absorption spectra were recorded using an Agilent Cary 60 UV-Vis spectrophotometer (Agilent Technologies, California, USA). The temperatures of spectroscopic measurements were maintained at 25 °C with an Agilent Peltier temperature controller accessory. A Desaga Uvis lamp was used for the UV light (366 nm) for the photographs (Jahnsdorf, Germany).

Synthesis of gold nanoclusters

Gold nanoclusters were synthesized using the method proposed by Zhang et al. [19] which utilizes glutathione for stabilization. Briefly, 10 mL of 10 mM $HAuCl_4$ and 10 mL 15 mM glutathione were mixed vigorously for 2 min. Then, 2 mL of 1 M NaOH was added to the mixture. Finally, the solution was stirred at 200 rpm at 37 °C for 24 h. The yellow solution of gold nanoclusters was washed to remove the excess glutathione followed by the addition of 80 mL of methanol. Then, the mixture was centrifuged at 9000 rpm for 20 min. The precipitates were dispersed in 20 mL of ultrapure water and kept under dark room conditions.

Synthesis of silver nanoclasters

The method described by Patrick et al. [20] was used for the synthesis of AgNC. 19 mg α-lipoic acid was added to 14 mL of ultrapure water followed by the addition of 7 mg $NaBH_4$ while stirring. After 30 min of stirring, a clear solution was obtained. Then, first 700 µL of 25 mM $AgNO_3$, then 2 mL of 0.13 M $NaBH_4$ were added. The flask was covered with an aluminum foil to keep it away from light. After stirring for 5 h, orange AuNCs were formed which were then stored at dark.

Hg^{2+} sensing in the solution phase

AgNCs were first diluted 1:4 with distilled water and AuNCs were directly used since their fluorescence signals were not intense. Analytes were prepared in water and were directly added to the clusters. All the fluorescence measurements were recorded at 25 °C by controlling the temperature using a Peltier accessory. Preliminary tests were performed by adding possible interferences to the nanoclusters and photographs were taken. by placing the analytes under white light and UV-light for colorimetric and fluorimetric responses. All titrations were performed using a stock solution of 10 µM $Hg(NO_3)_2$. Certified mercury standards were used as real samples.

Hg^{2+} sensing on glass fiber pads

Glass fiber pads were cut in the dimensions of 2 mm 8 mm. Time for immersion of pads in AgNC was optimized by measuring the fluorescence intensities at different times (5 s, 8 s, 10 s, 12 s, and 15 s). The pads were immersed in the AgNC solution for 8 s and left to dry at room temperature. Once the pads were dry, 12 µL of the blank solution and samples (1 nM, 10 nM, 100 nM, and 1000 nM Hg^{2+}) were pipetted onto pads and left to dry again. Then, photographs of the pads were taken under white and UV lights (366 nm).

RESULTS AND DISCUSSION

The reference methods report that AgNC (ϕ = ~5.0%) have higher quantum yield than AuNC (ϕ = ~1.5%). [19-20] This can clearly be observed in photographs taken under UV light (Figures 1a and 2a). Nevertheless, the effect of Hg^{2+} on fluorescence intensity can be easily observed for both nanoclusters even by naked eye. However, the colorimetric responses and UV-Vis absorption titrations reveal that the mechanism of Hg^{2+} sensing is different in these nanoclusters. While Hg^{2+} produces a colorimetric response in AgNC, which is indicated by the disappearance of yellow (Figure 1a), no colorimetric response is observed when Hg^{2+} is introduced to AuNC (Figure 2a). The colorimetric response obtained by AgNC can be quantified using the UV-Vis absorption spectra (Figure 1b). Fluorescence signals show similar responses to colorimetry in AgNC. When Hg^{2+} is introduced, the aggregation of AgNC can be observed by the disappearance of color and fluorescence quenching. The mechanism in Hg^{2+} sensing by AgNC can be the reduction of Hg^{2+} followed by the formation of Ag-Hg amalgam formation. In this study, these colorimetric and fluorimetric responses were monitored by time in the kinetic mode of a fluorescence spectrophotometer and it was found that the reaction occurred immediately

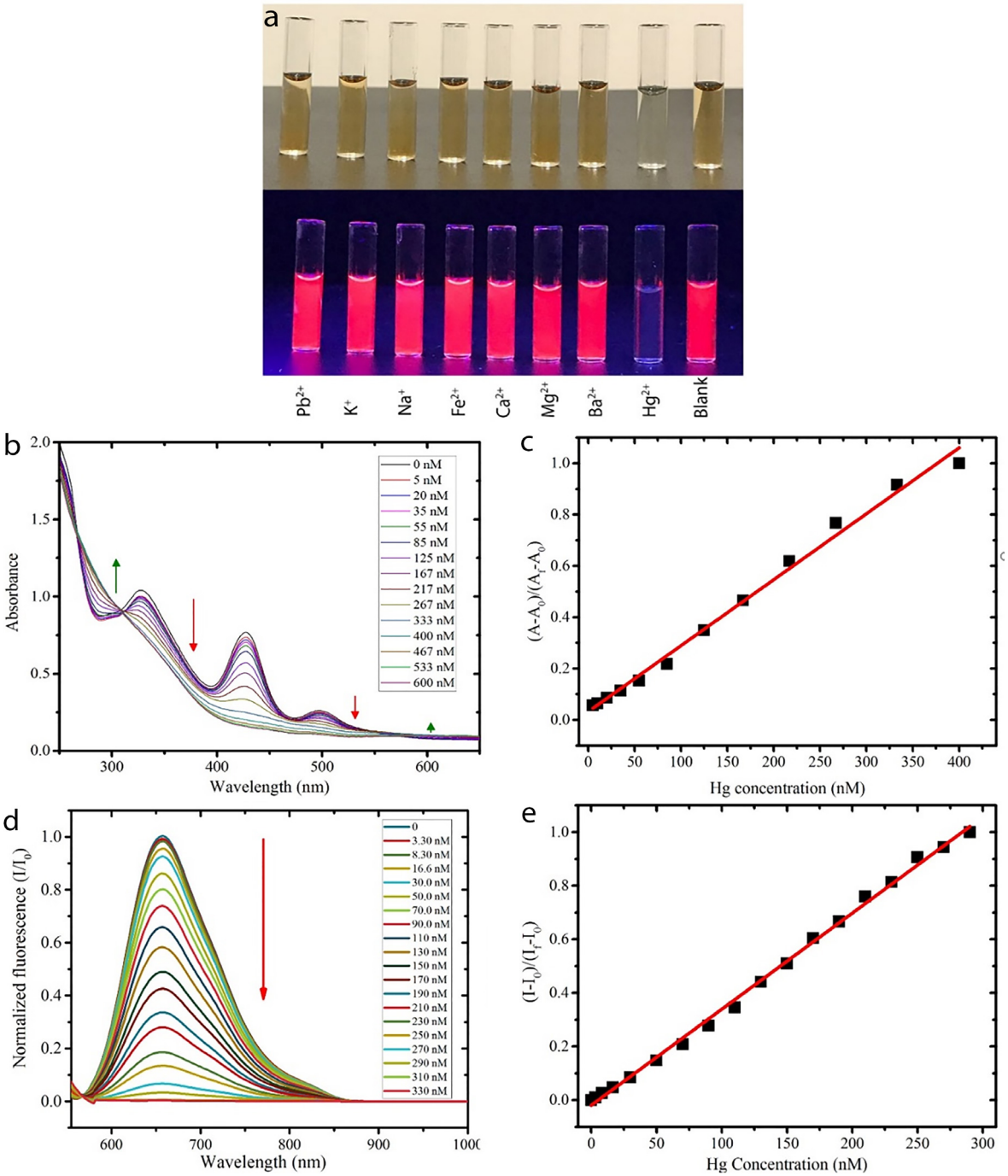


Figure 1. a) Naked eye detection of Hg^{2+} among some other cations using AgNC b) UV-Vis absorption titration spectra of Hg^{2+} and AgNC, c) Calibration curve for Hg^{2+} and AgNC UV-Vis titration, d) Fluorescence titration spectra of Hg^{2+} and AgNC e) Calibration curve for Hg^{2+} and AgNC fluorescence titration.

after the addition of Hg^{2+}.

Besides, the responses were concentration-dependent; thus, can be used in quantitative analysis. On the other hand, AuNC responded to the addition of Hg^{2+} in a different way. Although the absorbance spectrum of AuNC was not affected by Hg^{2+}, the fluorescence was quenched. In this case, the suggested mechanism was not the aggregation of AuNC, but it was probably the formation of a complex between Hg^{2+} and the carboxyl group of glutathione on the surface of AuNC. Then a photo-induced electron transfer from AuNC to Hg^{2+} complex might occur. This phenomenon can also be observed in some quantum dot-based sensing. [21]

In brief, colorimetric and fluorimetric responses were obtained from AgNC while only fluorimetric response was

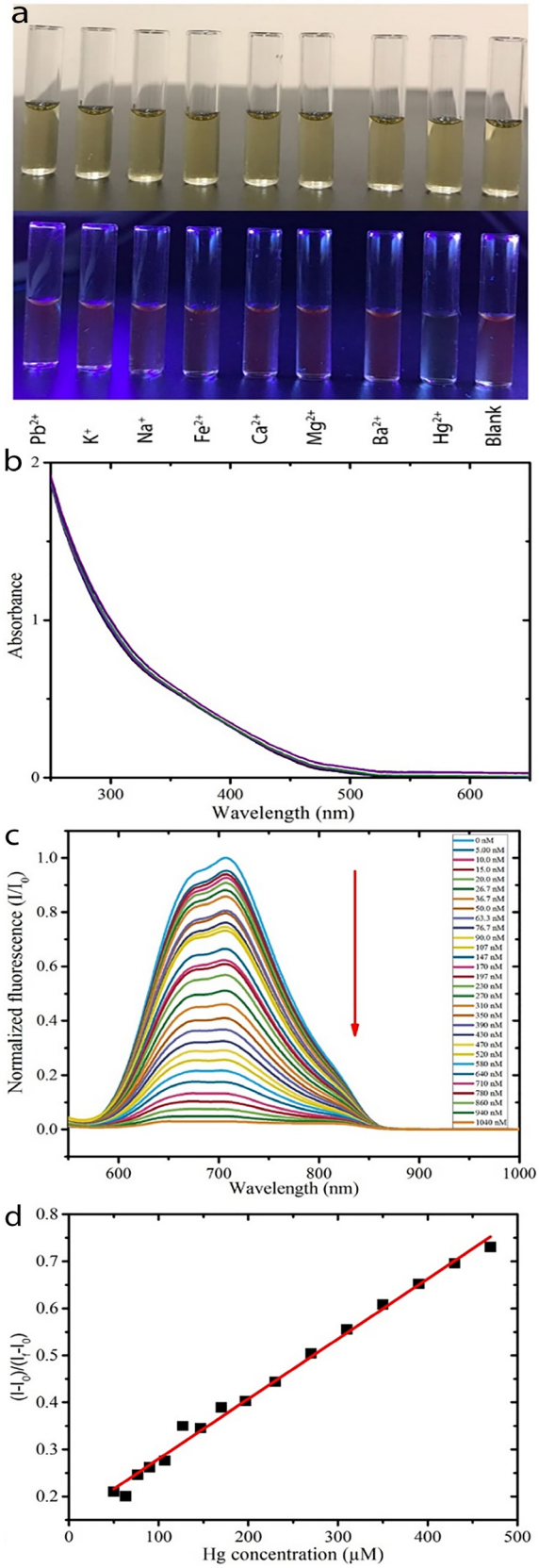


Figure 2. a) Naked eye detection of Hg^{2+} among some other cations using AuNC, b) UV-Vis absorption titration spectra of Hg^{2+} and AuNC, c) Fluorescence titration spectra of Hg^{2+} and AuNC d) Calibration curve for Hg^{2+} and AuNC fluorescence titration.

observed for AuNC. This creates a specific response pattern (Figure 3) for Hg^{2+} cation. The obtained response pattern increases the selectivity of Hg^{2+} sensing and is especially important in this type of sensor, which does not employ any analyte-specific agents. There is usually a contradiction between the selectivity and simplicity/cost-effectiveness of analytical methods. When an analytical method concentrates on high selectivity, its generally complexity and cost increase or vice versa. Thus, using two or more less selective sensors rather than expensive and highly selective analyte-specific agents (antibody, aptamer, etc) allows obtaining required information to analyze a sample. Here, only two simple nanoclusters were employed for Hg^{2+} sensing and they interacted with the analyte using different mechanisms; thus, selective sensing of Hg^{2+} was achieved following a very simple and cost-effective synthesis method. The effects of some selected metals were also followed under white light and UV-light and no interference was observed (Figures 1a and 2a).

Firstly, UV-Vis titrations were performed for both nanoclusters (Figures 1b and 2b). The responses from the AgNC-Hg^{2+} UV-Vis titration were used for quantitative determination (Figure 1c). Then, isosbestic points (312 nm and 539 nm) were determined from the UV-Vis spectra for the determination of the excitation wavelength in the fluorescence titration of AgNC and Hg^{2+}. Although the highest emission for AgNC was observed when it was excited at 432 nm, titrations were realized at an excitation wavelength of 539 nm since emission is independent from absorbance changes at isosbestic points, thus resulting in better correlation factors between Hg^{2+} and fluorescence quenching. Fluorescence of AgNC started to quench at around 1 nM Hg^{2+} and total quenching was achieved upon the addition of 330 nM Hg^{2+} to AgNC (Figure 1d). A linear correlation was observed between AgNC and Hg^{2+} (Figure 1e). On the other hand, fluorescence titration of AuNC and Hg^{2+} indicated a non-linear relationship in a wide range (Figure 2c). For this reason, the range of titration between 50-470 nM Hg^{2+} that showed a linear relationship was used for the calibration (Figure 2d). Both titrations were carried out in water at 25 °C. Some of the validation parameters

Table 1. Some method validation parameters for Hg^{2+} sensing

	Silver nanoclusters		*Gold nanoclusters*
	Fluorescence	*UV-Vis*	*Fluorescence*
Linear range (nM)	*3.3-290*	*5-400*	*50-470*
Detection limit (nM)	*1.04*	*1.65*	*1.84*
Quantitation limit (nM)	*3.16*	*5.00*	*5.59*
Slope	*0.003586*	*0.002571*	*0.001277*
Intercept	*-0.01913*	*0.03248*	*0.1520*
Coefficient of determination	*0.9974*	*0.9928*	*0.9922*

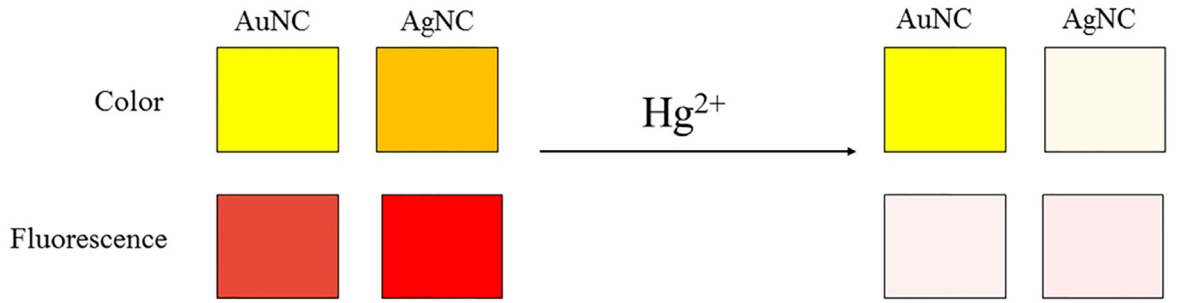


Figure 3. Optical response pattern obtained from nanoclusters

such as linear range, detection and quantification limits, and the coefficient of determination for both nanoclusters are given in Table 1. Finally, the certified mercury standard solutions were analyzed to test the accuracy and precision of the method. The results demonstrate high accuracy and precision at low levels of concentration (Table 2).

After analyzing the nanocluster-mercury interaction in the solution phase, the method was transferred to glass fiber pads which are commonly used in lateral flow immunoassay applications as sampling or conjugation pads. Here, the aim was to develop simple, user-friendly, cheap and disposable devices applicable to the on-site analysis of mercury. For this purpose, different types of paper such as chromatography paper, nitrocellulose absorbent pads and glass fiber pads were tested. As expected, the sensitivity of all materials was found to be lower compared to the solution-based method. Among these materials, the best performance in terms of sensitivity was obtained from glass fibers. This may be attributed to their higher sample absorption capacity and lower material density.

Small strips of glass fiber pads were immersed in AgNC to absorb the nanoclusters. The time taken for the pads for complete absorption were determined by studying the fluorescence of pads after keeping them in AgNC at different time intervals (5 s, 8 s, 10 s, 12 s, and 15 s). The results showed that pads were saturated with AgNC in 8 s and this condition was used in further experiments.

After solvent evaporation at room temperature, the fluorescence of AgNC in glass fiber pads under UV-light could be observed even by naked eye. Then, Hg^{2+} samples were applied to pads at different concentrations and the photographs of pads were taken using a mobile phone under sunlight and UV-light (Figure 4a). Although naked-eye detection of color change was difficult at lower concentrations (1 nM and 10 nM), the change was clearly seen at higher concentrations (100 nM and 1000 nM). On the other hand, it was easier to detect the change in fluorescence even at low concentrations. This is mostly because the red fluorescence of AgNC was not interfered with other lights. If the nanosensors had blue fluorescence, it would be difficult to apply this method since strong scattering of paper materials can suppress the blue fluorescence of sensor. Thus, another advantage of nanoparticles is that their optical properties can be easily modified to meet the requirements of sensing. For better quantification, the blue channel of the photo was removed and fluorescence intensities were measured using the Image J software. Considering the simplicity of the experimental setup and application, it can be concluded that the fluorescence intensity and Hg^{2+} concentration was correlated (Figure 4b) and this method can be used in the quantitative determination of Hg^{2+} in drinking water.

Table 2. Accuracy and precision of the Hg^{2+} sensing

Concentration of certified reference	*Found*	*Relative standard deviation (%)*	*Relative error (%)*
		Silver nanoclusters fluorescence measurements	
5.0 nM	*4.8 nM*	*2.54%*	*-3.38%*
50.0 nM	*49.0 nM*	*3.98%*	*-2.07%*
100.0 nM	*101.5 nM*	*1.71%*	*1.53%*
		Silver nanoclusters UV-Vis measurements	
10.0 nM	*10.6 nM*	*2.72%*	*6.21%*
100.0 nM	*101.5 nM*	*1.63%*	*1.49%*
200.0 nM	*202.9 nM*	*2.72%*	*1.46%*
		Gold nanoclusters fluorescence measurements	
60.0 nM	*61.7 nM*	*2.87%*	*2.78%*
120.0 nM	*122.4 nM*	*0.12%*	*2.03%*
240.0 nM	*236.7 nM*	*2.05%*	*-1.38%*

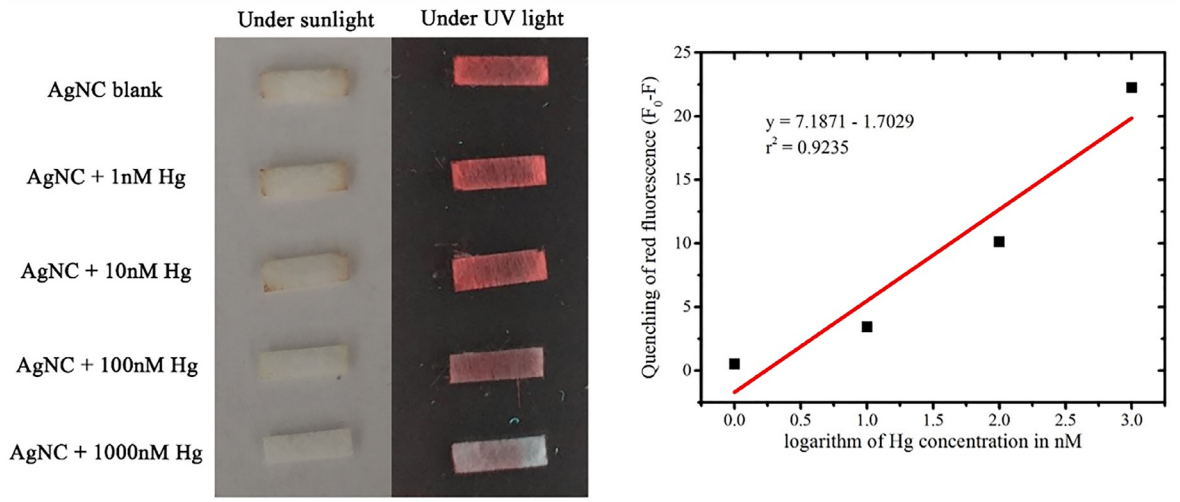


Figure 4. Photo of glass fiber pads under sunlight and under UV light (left) and the curve showing correlation between logarithm of Hg^{2+} concentration and fluorescence quenching.

CONCLUSION

In this study, sensitive and easy-to-use assays were developed for the determination of Hg^{2+} cation in water. Optical responses obtained after interactions between nanoclusters and Hg^{2+} were used in the analysis. Colorimetric and fluorimetric responses created a response pattern for the Hg^{2+} cation, which increases the selectivity of this simple method. The sensitive method was successfully applied to certified mercury standards. Finally, the proposed method based on AgNC was implemented in glass fiber pads to develop disposable, cheap, simple, portable, and sensitive devices. However, the fluorescence of AuNC was not sufficient for Hg^{2+} sensing by this simple setup since the quantum yield of AuNC was low. Therefore, further studies are needed to increase the quantum yield through the modification of AuNC.

REFERENCES

1. Counter SA, Buchanan LH, Ortega F, Laurell G. Elevated blood mercury and neuro-otological observations in children of the Ecuadorian gold mines. Journal of Toxicology and Environmental Health–Part A65 (2002) 149–163.
2. Ratcliffe HE, Swanson GM, Fischer LJ. Human exposure to mercury: A critical assessment of the evidence of adverse health effects. Journal of Toxicology and Environmental Health 49 (1996) 221–270.
3. Sweet LI, Zelikoff JT. Toxicology and immunotoxicology of mercury: A comparative review in fish and humans. Journal of Toxicology and Environmental Health–Part B–Critical Reviews 4 (2001) 161–205.
4. Branco V, Caito S, Farina M, Teixeira da Rocha J, Aschner M, Carvalho C. Biomarkers of mercury toxicity: Past, present, and future trends. Journal of Toxicology and Environmental Health – Part B: Critical Reviews (2017) 1–36.
5. de Souza SS, Campiglia AD, Barbosa Jr F. A simple method for methylmercury, inorganic mercury and ethylmercury determination in plasma samples by high performance liquid chromatography-cold-vapor-inductively coupled plasma mass spectrometry. Analytica Chimica Acta 761 (2013)11–17.
6. Fu L, Shi S-Y, Chen X-Q. Multi-element analysis of water decoction of medicine food homology plants using inductively coupled plasma-tandem mass spectrometry. Spectrochimica Acta Part B: Atomic Spectroscopy 133 (2017) 34–39.
7. Gu W, Pei X, Cheng Y, Zhang C, Zhang J, Yan Y, et al. Black Phosphorus Quantum Dots as the Ratiometric Fluorescence Probe for Trace Mercury Ion Detection Based on Inner Filter Effect. ACS Sensors 2 (2017) 576–582.
8. Zhang JR, Huang WT, Zeng AL, Luo HQ, Li NB. Ethynyl and Ⓟ-stacked thymine-Hg^{2+}-thymine base pairs enhanced fluorescence quenching via photoinduced electron transfer and simple and sensitive mercury ion sensing. Biosensors and Bioelectronics 64 (2015) 597–604.
9. Liu Y-M, Zhang F-P, Jiao B-Y, Rao J-Y, Leng G. Automated dispersive liquid-liquid microextraction coupled to high performance liquid chromatography – cold vapour atomic fluorescence spectroscopy for the determination of mercury species in natural water samples. Journal of Chromatography A 1493 (2017) 1–9.
10. Ren W, Zhang Y, Chen HG, Gao ZF, Li NB, Luo HQ. Ultrasensitive Label-Free Resonance Rayleigh Scattering Aptasensor for Hg^{2+} Using Hg^{2+}-Triggered Exonuclease III-Assisted Target Recycling and Growth of G-Wires for Signal Amplification. Analytical Chemistry 88 (2016) 1385–1390.
11. Botasini S, Heijo G, Méndez E. Toward decentralized analysis of mercury (II) in real samples. A critical review on nanotechnology-based methodologies. Analytica Chimica Acta 800 (2013) 1–11.
12. Ding Y, Wang S, Li J, Chen L. Nanomaterial-based optical sensors for mercury ions. TrAC Trends in Analytical Chemistry 82 (2016) 175–190.
13. Xu X, Li Y-F, Zhao J, Li Y, Lin J, Li B, et al. Nanomaterial-based approaches for the detection and speciation of mercury. Analyst 140 (2015) 7841–7853.

14. Farhadi K, Forough M, Molaei R, Hajizadeh S, Rafipour A. Highly selective Hg2+ colorimetric sensor using green synthesized and unmodified silver nanoparticles. Sensors and Actuators B: Chemical 161 (2012) 880–885.
15. Katok KV, Whitby RLD, Fukuda T, Maekawa T, Bezverkhyy I, Mikhalovsky SV, et al. Hyperstoichiometric Interaction Between Silver and Mercury at the Nanoscale. Angewandte Chemie International Edition 51 (2012) 2632–2635.
16. Ono A, Togashi H. Highly Selective Oligonucleotide–Based Sensor for Mercury(II) in Aqueous Solutions. Angewandte Chemie International Edition 43 (2004) 4300–4302.
17. Li H, Zhang Y, Wang X, Gao Z. A luminescent nanosensor for Hg(II) based on functionalized CdSe/ZnS quantum dots. Microchimica Acta 160 (2008) 119–123.
18. Diez I, Ras RHA. Fluorescent silver nanoclusters. Nanoscale 3 (2011)1963–1970.
19. Zhang H, Liu Q, Wang T, Yun Z, Li G, Liu J, et al. Facile preparation of glutathione–stabilized gold nanoclusters for selective determination of chromium (III) and chromium (VI) in environmental water samples. Analytica Chimica Acta 770 (2013) 140–146.
20. Chin PTK, van der Linden M, van Harten EJ, Barendregt A, Rood MTM, Koster AJ, et al. Enhanced luminescence of Ag nanoclusters via surface modification. Nanotechnology 24 (2013) 075703/1–/7, 7 pp.
21. Shang ZB, Wang Y, Jin WJ. Triethanolamine–capped CdSe quantum dots as fluorescent sensors for reciprocal recognition of mercury (II) and iodide in aqueous solution. Talanta 78 (2009) 364–369.